International Journal of Fracture **123:** 177–185, 2003.

Size effect on the fracture toughness of metallic foil

HUAI-WEN WANG, YI-LAN KANG*, ZHI-FENG ZHANG and QING-HUA QIN
School of Mechanical Engineering, Tianjin University, Tianjin, 300072, P. R. China
*(*Author for correspondence: Fax: +86-22-87401572; E-mail: ylkang@public.tpt.tj.cn)*

Abstract. The size effects on fracture behavior of Cu foil are investigated by a new optical technique, the digital speckle correlation method (DSCM). Displacement and strain fields around a crack tip are analyzed for different thicknesses of Cu foil. Then, the J integral and fracture toughness J_C are evaluated directly from the strain fields around the crack tip. The fracture toughness J_C is obtained as a function of foil thickness. The results indicate that J_C indeed depends on foil thickness within a certain range of thickness (the thickness varies from 20 micron to 1 millimeter in this work).

Key words: Deformation fields, digital speckle correlation method, fracture toughness, metallic foil, size effect.

1. Introduction

There has been an increasing application for metallic foil due to the rapid development of communication and microelectronics technology, especially microelectro-mechanical systems and integrated circuits. The foils are essential structural components in those microsystems. The reliable mechanical properties of these foils especially fracture behaviors, as the possibility of crack development is inevitable during the service life of the foil, are critical to the safety and functioning of these microdevices and should be accurately determined. Several works has been done for thin foil in last several years. For fatigue problems, Hong and Weil (1996) proved that the properties of two electroplated and one wrought foil obeyed the Basquin equation, and there was no difference between the fatigue properties of thin foil and bulk-wrought copper. Merchant et al. (1999) corroborated the above findings for a variety of electrodeposited foils in the thickness range of 12 μm to 35 μm. Read (1998) investigated the resistance of copper thin-film to failure by tension-tension fatigue. He found that the dislocations associated with the plastic strain traverse the specimen in a direction at approximately a 45° angle to both the load axis and the through-thickness direction by a transmission electron microscope. Recently, Hadrboletz et al. (2001) studied the fatigue crack growth and associated fracture processes of foils with thickness ranging from 20 μm to 250 μm, using the electron channeling contrast imaging-technique in a scanning electron microscope. They found that a size effect may be observed if the ratio of grain size to foil thickness is close to or larger than unity and the constitutive length scale of the apparent plastic strain gradient is a considerable portion of the foil thickness. Pardoen et al. (1999) have investigated experimentally and numerically the size effect on the fracture toughness of aluminum thin plates of 1–6 mm thickness from tensile testing of cracked DENT (double edge notched tension) specimens. Their research show that the thickness indeed influence the fracture toughness in a certain thickness region and the critical J-integral and critical CTOD etc. constitute equivalent measures of fracture toughness at small thickness. However, as to fracture behaviors of metallic foils little work

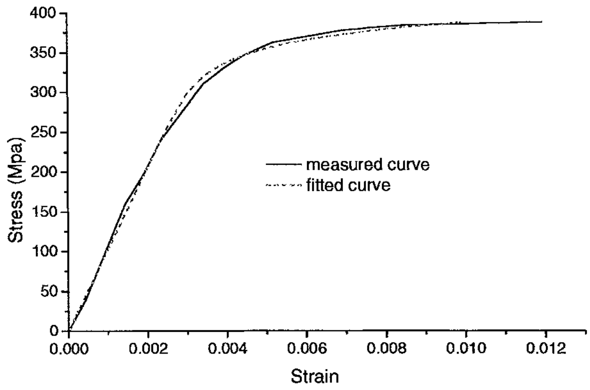

Figure 1. Stress-strain curve of the material.

has been reported in the literature. Perhaps this is due to the difficulties in accurately testing the deformation and strain fields for foil in the crack tip region. Up to now, it has not been founded in literature that the displacement and strain fields of the thin foil in crack tip are tested by effectual experimental method. So it is necessary to look for a useful experimental technique in this field.

The purpose of this paper is to explore the fracture behavior of foils and reveal the size effect of the fracture problem by a new optical experimental means that can get the deformation fields (displacement and strain) in the crack tip region and give a quantitative curve of the $J_c(t)$ (t – thickness) for a kind of the copper foil material. In this present, the digital speckle correlation method is used to study the fracture behavior of foil. Displacement and strain fields around the crack tip are measured. The J integral can then be calculated from the measured strain field. Fracture toughness J_C of specimens with a thickness range from 20 μ to 1 mm are evaluated. Finally, the effect of foil thickness on fracture toughness is analyzed and some conclusions are drawn.

2. Experimental procedure

2.1. Specimen

The specimens used in the test were all made of T2 Cu foil that was produced by the Shanghai smeltery and with the same materials components and the same processing technology. Their thickness range was from 20 μ to 1 mm. The Young's modulus E and Poisson ratio μ of the material were about 108.5 GPa and 0.334, respectively. The uniaxial stress-strain curve, which was measured by the CSS-44100 experimental machine, is shown in Figure 1. From the curve we can see that this material is like a kind of power-hardening material. For power-hardening materials the uniaxial stress-strain curve can be described by the Ramberg–Osgood relation:

$$\frac{\varepsilon}{\varepsilon_0} = \frac{\sigma}{\sigma_0} + \alpha \left(\frac{\sigma}{\sigma_0}\right)^n, \tag{1}$$

where α is a coefficient and n is an exponent of the power hardening material, σ_0 and ε_0 are the flow stress and strain, respectively. Modeling the Ramberg–Osgood equation on this curve by the least square method, we obtain $n = 15.47$ and $\alpha = 0.0288$. From Figure 1 we can see that the fitted curves of the Ramberg–Osgood equation and the original stress-strain relation are in

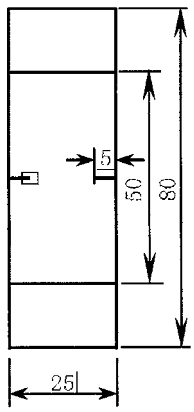

Figure 2. Dimensions of the specimen and the cracks.

a good agreement. The different thickness foil materials were made into double-edge cracked specimens. Its dimensions are shown in Figure 2. The crack on each specimen whose path was perpendicular to the rolling direction was made as fellows,firstly we used line-incise with a radius of 0.1 mm to make a initiatory crack and then used a sharp razor to make the crack tip. The radius of razor is approximately 25 μm. The validity of this pre-cracking method has been justified by Pardoen et al. (1999).

2.2. Experimental method

The digital speckle correlation method, which has been described elsewhere (Bruck et al., 1989; Wang et al., 2002; Kang et al., 2002), is used to investigate the size effect on fracture toughness in foils. In the test, random speckles on the specimen surface were produced to obtain a speckle pattern, as shown in Figure 3. Information for displacement and strain fields could be obtained by recording, digitizing and comparing speckle patterns on the specimen in different deformation states, especially those made before and after deformation. The difference between any two-pattern subsets contains the distortional information of the specimen. By using this information, the displacement and strain fields could be calculated by a mathematical calculation process described below.

The criterion for comparing two subsets is commonly given by using the cross-correlation coefficient. The cross-correlation coefficient for the two subsets can be written in discrete form as

$$C = \frac{\Sigma f(x, y) \cdot g(x^*, y^*)}{\sqrt{\Sigma f^2(x, y) \cdot \Sigma g^2(x^*, y^*)}}, \tag{2}$$

where (x, y) and (x^*, y^*) are Cartesian coordinates of a material point in the subsets of the non-deformed and deformed patterns, respectively. $f(x, y)$ and $g(x^*, y^*)$ are light intensities at that point in the corresponding subsets. The correlation coefficient C shows how closely the two subsets are related, with $C = 1$ corresponding to perfect correlation. In general, the maximum of C implies the coincidence of the assumed displacement and strain values with the actual deformation components.

In order to obtain the maximum of C, the following iterative formula is employed:

$$\boldsymbol{X}_{i+1} = \boldsymbol{X}_i - h\boldsymbol{H}_i\boldsymbol{g}_i, \tag{3}$$

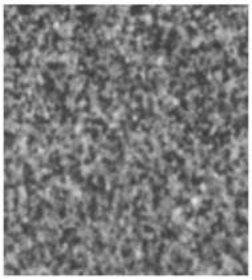

Figure 3. A typical speckle pattern.

where $\boldsymbol{X} = (x_1, x_2, x_3, x_4, x_5, x_6)^T = (u, v, \partial u/\partial x, \partial u/\partial y, \partial v/\partial x, \partial v/\partial y)^T$ are variables that describe the deformation. Scalar quantity h is the step size of iteration. Matrix $\boldsymbol{H}_i$ is the counterpart of the Hessian matrix and $\boldsymbol{g}_i$ is the Jacobian vector. When the maximum of C is obtained, the corresponding $\boldsymbol{X}$ is the distortional information of that point.

3. Results and discussion

In this section, the deformation fields around the crack tip are measured by the DSCM. The J integral and fracture toughness J_C are calculated directly from the strain field obtained from the experiment. Some discussion follows.

3.1. Deformation fields around crack tip

Displacement and strain fields over the crack tip region play an important role in analyzing the fracture behavior and calculating fracture toughness of a cracked specimen. They can be obtained by recording and comparing speckle patterns produced before and after deformation as well as analyzing them by the digital correlation technique described in the previous section. Figures 4 and 5 show distributions of the displacement $v(x, y)$ and the normal strain $\varepsilon_y(x, y)$ over the crack tip region under different loads. It can be seen from the figures that the DSCM can measure the deformation fields around the crack tip under different load levels.

3.2. Fracture toughness

In elasto-plastic fracture mechanics, the fracture criterion of foils is based on the energy release rate, J integral. The J integral criterion has successfully been used to solve many practical fracture problems. Therefore in this work we use fracture toughness J_C , the critical value of J integral, for analyzing the fracture behavior of foil.

The J integral in a nonlinear elastic material is defined by

$$J = \int_\Gamma \left(w \, \mathrm{d}y - T_i \frac{\partial u_i}{\partial x} \mathrm{d}s \right), \tag{4}$$

where Γ is an anticlockwise curve that surrounds the crack-tip, w is the strain energy density, T_i is a component of the traction vector, u_i is a component of the displacement vector.

In order to apply the DSCM to calculate J integral, expression (4) is rewritten as

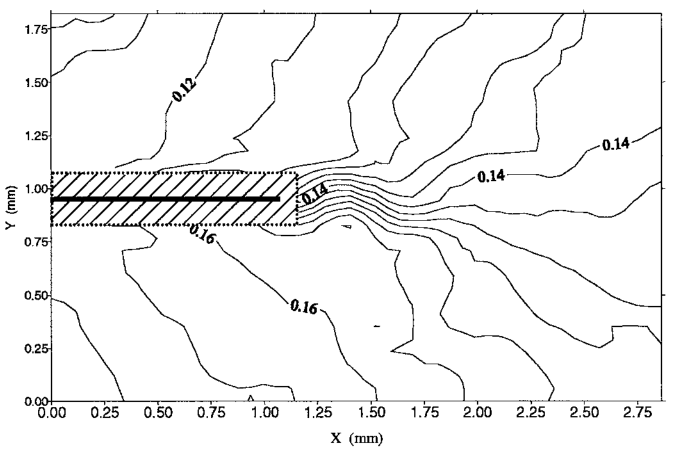

(a)

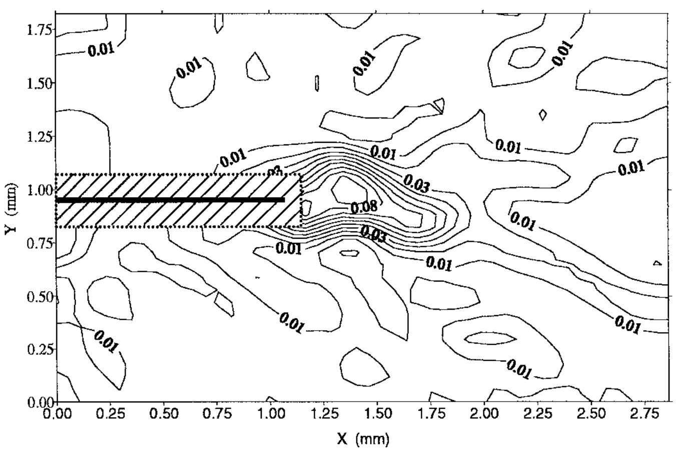

(b)

Figure 4. Distribution of displacement field and strain field at the crack tip ($P = 155.1$N). (a) Contour of displacement V field. (b) Contour of strain ε_y field.

$$
\begin{aligned}
J = {} & \frac{1}{2}\int_\Gamma \left[\frac{E}{1-\mu^2}\left(\frac{\partial u}{\partial x} + \mu\frac{\partial v}{\partial y}\right)\frac{\partial u}{\partial x} + \frac{E}{1-\mu^2}\left(\frac{\partial v}{\partial y} + \mu\frac{\partial u}{\partial x}\right)\frac{\partial v}{\partial y} + G\left(\frac{\partial u}{\partial y} + \frac{\partial v}{\partial x}\right)^2 \right] \mathrm{d}y \\
& - \int_\Gamma \left[\frac{E}{1-\mu^2}\left(\frac{\partial u}{\partial x} + \mu\frac{\partial v}{\partial y}\right)\frac{\partial u}{\partial x} + G\left(\frac{\partial u}{\partial y} + \frac{\partial v}{\partial x}\right)\frac{\partial v}{\partial x} \right] \mathrm{d}y \\
& + \int_\Gamma \left[\frac{E}{1-\mu^2}\left(\frac{\partial v}{\partial y} + \mu\frac{\partial u}{\partial x}\right)\frac{\partial v}{\partial x} + G\left(\frac{\partial u}{\partial y} + \frac{\partial v}{\partial x}\right)\frac{\partial u}{\partial x} \right] \mathrm{d}x.
\end{aligned}
\tag{5}
$$

In our calculation, the integral path forms a symmetrical rectangle as shown in Figure 6. Thus, J can also be written in the form

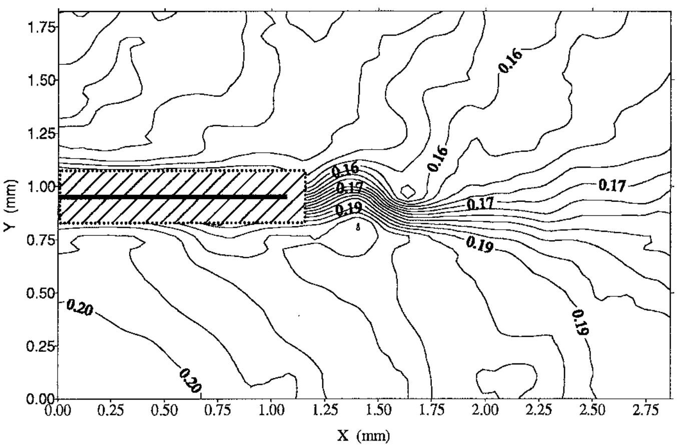

(a)

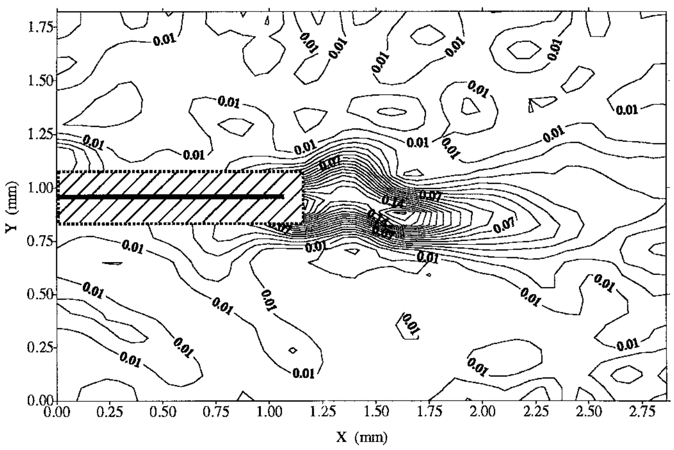

(b)

Figure 5. Distribution of displacement field and strain field at the crack tip ($P = 188.1$N). (a) Contour of displacement V field. (b) Contour of strain ε_y field.

$$J = J_{(1)} + J_{(2)} + J_{(3)} + J_{(4)} + J_{(5)}, \tag{6}$$

where $J_{(i)}$ stands for the value of J integral along the path i (see Figure 6). With Equation (6), the J integral can be calculated by way of the digital correlation data.

In this test, a double CCD (charge coupled device) system equipped with zooms, as shown in Figure 7, was designed to accurately determine the value of J_C , i.e., J integral when the crack tip initiates. One CCD system was used to observe the crack tip in real-time and another to capture digital speckle pattern in serially. The pattern captured just before the crack tip initiation was taken as the deformed image. It is well-known that one important requirement of any fracture toughness test is the ability to detect the initiation of fracture. There are several methods has been proposed in the literature. Here we refer to the method given by E-Isoudani

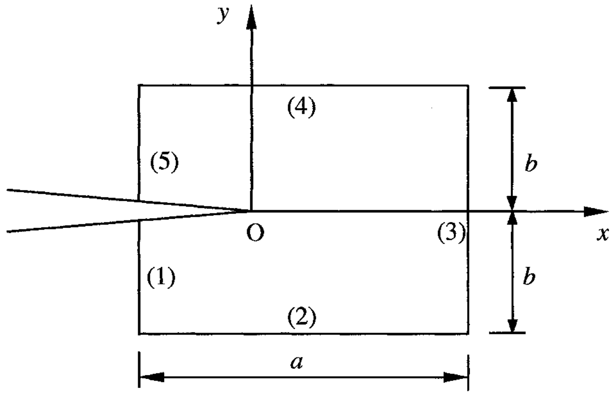

Figure 6. Rectangular symmetrical integral path.

Table 1. Calculated results of J_C.

Thickness (mm)		0.002	0.003	0.05	0.1	0.2	0.3	0.4	0.6	0.8	1.0
J_C	No. 1[a]	4.78	6.42	7.22	17.75	22.78	36.73	24.89	16.54		12.19
($\mathrm{N\,mm^{-1}}$)	No. 2	5.89	5.59	6.55	18.14	24.78	33.61	27.21	18.41	15.83	12.27
	No. 3	4.378	6.13	6.22	17.92	21.74	32.97	25.85	16.32	15.54	10.83
	No. 4	4.09	7.55	8.89	17.19	21.86	32.73	26.61	19.18	14.09	12.37

[a] No. i stands for specimen $i(i = 1, 2, 3, 4)$

(1990), namely thumbnails technique, because the precision of this technique is high enough for our experimental purpose and can be used in the experimental research step by step. Moreover, it has been used by many researchers in the literature. And then the DSCM was used to analyze the deformation and the J integral was calculated using Equation (6). As the captured speckle pattern was related to the crack initiation, the calculated J integral was considered as the critical value of J integral, i.e., J_C. In order to study the effect of thickness on J_C, specimens with thickness $h = 0.02$, 0.03, 0.05, 0.1, 0.2, 0.3, 0.4, 0.6, 0.8 and 1 mm were used in our test, and each thickness was repeated four times. The values of J_C corresponding to these specimens are listed in Table 1 and Figure 8. The figure is similar to plots presented in many textbooks (Kanninen, 1985). However, most of them have no quantitative results and provide a qualitative analysis only.

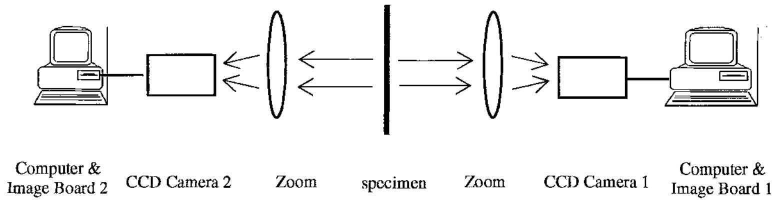

Figure 7. Double CCD system.

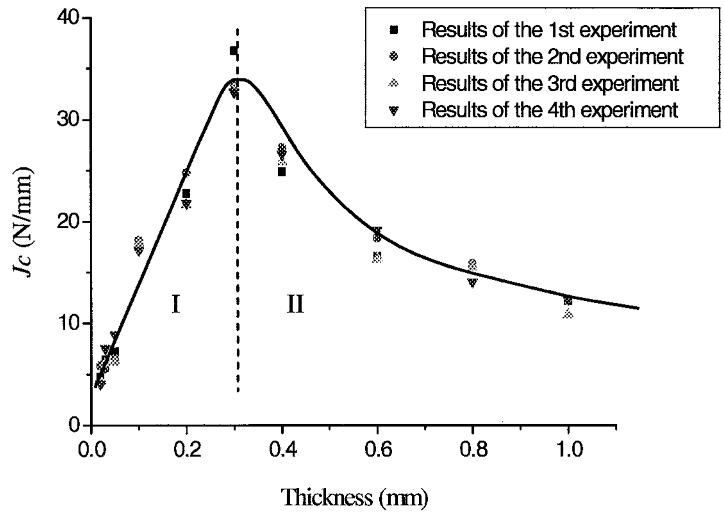

Figure 8. Relation between J_C and thickness.

3.3. Discussion

It can be seen from Figure 8 that the fracture toughness J_C indeed depends on thickness in a certain thickness range, say between 0.02and 1 mm in this work. This may be attributed to certain factors, such as energy spent in the neck shrinking process, inner and surface micro-defects, stress triaxiality ratio, etc. The contributions of these factors to fracture toughness may be different for different foil thicknesses.

For small thicknesses ($h \leqslant 0.3$ mm), the resistance of fracture initiation is similar to that of fracture propagation because neck shrinkage is almost fully developed just before crack initiation. As fracture toughness is related to the energy spent in the neck shrinking process in front of the crack tip, and the energy depends on the thickness of the specimen, fracture toughness varies with thickness. When the thickness is less than or equal to 0.3 mm, fracture toughness increases rapidly along with the increase of thickness until it reaches maximum. Conversely, when the thickness is greater than 0.3 mm, fracture toughness decreases gradually along with the increase of thickness (see Figure 8).

It should be pointed out that micro-defects and heterogeneity of microstructure are also major factors affecting fracture toughness because they may induce a large stress concentration when the foil is thin. This weakens the fracture resistance of material; therefore fracture toughness decreases rapidly with the decrease of thickness. With an increase of thickness, the effect of these factors diminishes. The fracture resistance ability of the material is strengthened, i.e., fracture toughness increases until it reaches its maximum. The stress state is gradually converted from plane stress to plane strain when the thickness is greater than 0.3 mm. At this stage, the effects of micro-defect and heterogeneity on fracture toughness become increasingly weaker with the increase of thickness. However, with the increase of thickness, the stress triaxiality ratio increases in such a way that it may strongly constrain deformation. As a result of this the initiation of the crack occurs well before the steady state of necking. Therefore for very thick specimens fracture toughness decreases with the increase of thickness until it reaches its plane strain state.

4. Conclusion

The fracture behavior of Cu foils is investigated experimentally by the DSCM in this paper. The displacement and strain fields near the crack tip are measured by the DSCM and their contour maps are obtained. Based on the experimental results and the concept J_C, size effect on fracture toughness of foils is discussed in detail. Experimental results indicate that J_C depends strongly on thickness of foil within a certain range of thickness. The study shows that the energy spent in the neck shrinking process in front of the crack tip, micro-defects of the material, and the stress triaxiality ratio may be the major factors affecting fracture behavior, and their contributions to fracture toughness will vary with different thickness of foil. Experimental results also indicate that the digital speckle correlation method is a promising test technique in studying the fracture behavior of low-dimensional materials.

Acknowledgement

This work was supported by the National Natural Science Foundation of China (Grant no.: 10232030 and key international co-operation project) and the support is gratefully acknowledged.

References

Bruck, H.A., McNeill, S.R., Sutton, M.A. and Peters, W.H. (1989). Digital image correlation using Newton-Raphson method of partial differential correction. *Experimental Mechanics* **29**, 261–267.

EI-Soudani, S.M. (1990). Quantitative fractography and fracture mechanics characterization. *Journal of the Minerals. Metals and Materials Society* **42**(10), 20–27.

Hadrboletz, A., Weiss, B. and Khatibi, G. (2001). Fatigue and fracture properties of thin metallic foils. *International Journal of Fracture* **107**, 307–327.

Hong, S. and Weil, R. (1996). Low cycle fatigue of thin copper foils. *Thin Solid Films* **283**, 175–181.

Kang, Y.L., Fu, D.H., Wang, H.W. and Lu, Z.X. (2002). Analysis of experiment on mechanical properties of thin foils. In: *3rd International Conference on Experimental Mechanics*, (Edited by Xiaoping Wu, Yuwen Qin, Jing Fang, Jingtang Ke) *Proceedings of SPIE* **4537**, 35–40.

Kanninen, M.F. and Popelar C.H. (1985). *Advanced Fracture Mechanics*, Oxford University Press, New York.

Merchant, H.D., Minor, M.G. and Liu, Y.L. (1999). Mechanical fatigue of thin copper foil. *Journal of Electronic Materials* **28**, 998–1007.

Pardoen, T., Marchal, Y. and Delannay, F. (1999). Thickness dependence of cracking resistance in thin aluminum plates. *Journal of the Mechanics and Physics Solids* **47**, 2093–2123.

Read, D.T. (1998). Tension-tension fatigue of copper thin films. *International Journal of Fatigue* **20**, 203–209.

Wang, H.W. and Kang, Y.L. (2002). Improved digital speckle correlation method and its application in fracture analysis of metallic foil. *Optical Engineering* **41**, 2793–2798.